9. Fighting the Influenza A virus. New scaffolds and therapeutic targets

Marta Barniol-Xicota and Santiago Vázquez

Laboratori de Química Farmacèutica (Unitat Associada al CSIC), Facultat de Farmàcia i Ciències de l'Alimentació, and Institute of Biomedicine (IBUB),Universitat de Barcelona, Av. Joan XXIII, s/n, Barcelona E-08028, Spain

Abstract. Influenza A virus is a major threat to human health and a potential biowarfare pathogen. The M2 proton channel protein, essential for virus viability, contains a single transmembrane domain that forms a homo-tetrameric pore, targeted by Amantadine. The emergence of resistance to drugs poses major health risk as most of Influenza virus isolates are now Amantadine-resistant. Although only a handful of mutations are tolerated in transmissible viruses, V27A, S31N and L26F, they are enough to jeopardize public health. Aiming to overcome drug resistance, we are preparing new polycyclic small molecules which putatively will inhibit the wild-type and the mutant M2 channels.

1. The Influenza A virus

The influenza A virus, commonly known as the Flu virus, is a coated virus of the *Orthomyxoviridae* family, which has a multipartite, negative-sense,

Correspondence/Reprint request: Dr. Marta Barniol-Xicota, Laboratory of Chemical Biology, Department of Cellular and Molecular Medicine, KU Leuven, Herestraat 49, box 802, 3000 - Leuven, Belgium. E-mail: marta.barniolxicota@kuleuven.be
Dr. Santiago Vázquez, Laboratori de Química Farmacèutica (Unitat Associada al CSIC), Facultat de Farmàcia i Ciències de l'Alimentació, and Institute of Biomedicine (IBUB),Universitat de Barcelona, Av. Joan XXIII, s/n, Barcelona E-08028, Spain. E-mail: svazquez@ub.edu

single-stranded RNA genome that codes for 11 viral proteins. From the exterior to the interior of the virus, we find the following proteins: the hemagglutinin (HA) and the neuraminidase (NA), which are antigenic glycoproteins found in the lipid membrane of the virus; the M2 protein, which crosses the lipid coating in the form of a proton selective channel. In the viral interior, we find the nucleoprotein (NP), the matrix protein M1, the viral polymerase complex formed by the PA, PB1 and PB2, subunits, the non-structural protein NS1 and the nuclear export protein (NEP) [1].

The standard nomenclature of the viral strains includes: viral type/ specie from isolation (in case of non-human)/ isolation place/ number of isolate/ year of isolation/ hemagglutinin type/ neuraminidase type [2]. For example A/Panama/2007/1999(H3N2) indicates an Influenza A virus found in humans in Panama, that is the number of isolate 2007 of the year 1999 and that has a HA type 3 and a NA type 2.

The two most relevant traits of the Influenza A virus are its high infectivity, which is responsible for its easy transmission through the airborne route or via hands-mouth, and its ability to mutate [3]. The viral mutations occur through two mechanisms: the antigenic drift, which consists in point mutations in the viral structure, that allow a slight variation of the viral properties and is responsible, for example, of the drug resistance mechanism. The other mutation path is the antigenic shift, which consists in the genetic rearrangement between two or more different influenza A viral strains, giving place to a new strain with mixed properties. For example, through this mechanism, an animal virus can acquire the capacity to infect humans [4].

2. The viral cycle

Viral entry. The cycle starts when the virus enters in the organism and recognizes the sialic acids located on the surface of the host's respiratory system epithelial cells, to which is attached thanks to the surface protein HA [5].

Endocytosis. Following, the virus enters into the cells through a receptor-mediated endocytosis, usually by clatrine, even alternative internalization routes as macropinocytosis [6] have been reported. The virus, hence, is internalized in a primary endosome with a pH around 6.

Fusion. The primary endosome is transported giving place to a late endosome in which the pH is again lowered thanks to the vacuolar ATPase (V-ATPase). This promotes an irreversible conformational change of the

HA, in which the N-terminus of the HA2 subunit, known as fusion peptide [7-8], is expelled. This fusion peptide will be inserted in the endosomal membrane, giving place to the fusion of both membranes, the viral and the endosomal one. The same pH shift also activates the M2 channel, which starts conducting protons, acidifying the viral interior. This will give place to the dissociation of the M1 protein from the viral ribonucleoprotein complex (vRNP), allowing the release of the vRNP to the cytoplasm from where they will be imported to the nuclei through the nuclear import factors. On another hand, the M1 protein will complex in late endosomes to be, in a similar way, imported to the nuclei [9].

Viral replication and transcription. Once in the nuclei the viral polymerase catalyzes the synthesis of one copy in positive sense of the viral RNA – the so-called complementary RNA, which will be copied to produce big quantities of viral RNA (vRNA) and the synthesis of a messenger RNA, of positive sense. The new vRNA will be encapsulated by the nucleoprotein and thanks to the NEP, the nuclear export complex will be formed; this will allow the crossing of one of the nucleoproteins to the cytoplasm. On another side, the mRNA will attach to the nucleoprotein to be exported through the nuclear export factor 1 (NXF1), which is the machinery that the host cell uses for its own RNA.

Translation. The mRNA highjacks the host cell translation mechanisms thanks to the NS1 protein, avoiding the response mechanisms of the host [10]. Once released from the NP, the mRNA are translated for viral proteins in the ribosomes. The NP, NS1, NEP and the M1 protein return to the nuclei to give place to more viral RNA. In contrast the NA, HA and the M2 protein will be transported to the endoplasmic reticulum and the Golgi apparatus where post-translational modifications will take place, giving mature proteins. Worthy of mention, during the transit through the Golgi apparatus – which has an acidic pH – the M2 protein is responsible of increasing the pH in the interior of the transport vesicles, to avoid the HA conformational change [11].

Packaging, virion formation and release of mature virus. Once the maturation process of the surface proteins HA, NA and the transmembrane protein M2 are completed, those proteins aggregate in the plasma membrane lipid rafts. Following, the viral RNA will attach to the HA, thanks to the action of the M1 protein. The high concentration of HA and NA, will alter the membrane curve, allowing the polymerization of the protein M1, in order to continue with the formation of the new virion. Simultaneously the M2 protein passes to the neck of this virion, altering

once again the plasma membrane, until this is separated from the virion [12] which will remain attached to the host cell uniquely by bonds of the HA with the sialic acid receptors. Finally, thanks to the scission of this bond by the NA, the newly formed influenza virus will be released [13].

As can be deduced from the viral cycle, all the Influenza A proteins play a paramount role. Hence, the malfunction or inhibition of any of those, will allow stopping the infection; consequently, all of them are subject to be used as anti-influenza A drug targets [14].

3. The M2 channel

3.1. Structure

The M2 viroporin of the Influenza A virus is a 97 amino acid transmembrane protein that assembles in tetramers to give place to a channel across the viral membrane. Each strand consists in two α-helixes with a left-handed parallelism respect the *N*-terminal region. This deviation is due to a slight tilt of 30-35º nearby the Gly 34 [15]. The following regions can be distinguished in each strand:

Residues 1 to 24 − N-terminus: Extracellular unstructured region, which function is the incorporation of the protein into the virion.

Residues 25 to 46 − Transmembrane domain [16]: Tetramer of α-helixes, which is responsible for the proton conduction. The drug-binding site is located in this region.

Residues 47 to 61 − Amphipathic cytoplasmic region: Intracellular, α helix structured domain that is responsible for the stabilization of the M2 protein and the release and scission of the newly formed virions.

Residues 62 to 97 − C-terminus: Intracellular unstructured region where the interaction with the matrix viral protein M1 takes place [17].

Since the structure of the M2 protein was solved in 2008 − by solution NMR [18] and X-Ray crystallography [19] - up to 15 different structures can be found in the Protein Data Bank (PDB). Nevertheless was not until 2014 that the M2 was assessed as a 2-fold symmetric tetramer, which can be better described as a dimerization of functional dimers [20-21].

3.2. Function

The main function of the M2 channel is to allow the proton flow in a controlled manner [15]. It acts as a pH regulator in order to allow, during the viral life cycle: i) the *proton diffusion to the interior of the endosome*,

where the virus is contained to reach a mature state, allowing the fusion of the viral membrane in the endosome and the right unpacking of the viral genome of the protein M1 [22] and, ii) the *delay of the acidification of the transport vesicles* in the Golgi apparatus to ensure the correct formation and the later release of the virus [23].

The transmembrane domain of the channel (residues 25 – 46) is the functional unit, as it contains the essential residues for the proton conduction. These are: the histidines in position 37 (**His37**), the pKa of which controls the conduction rate [24-25]; the tryptophans in position 41 (**Trp41**), which ensure the unidirectional proton flow [26]; the valine in position 27 (**Val27**), which forms a small valve to control the proton entrance to the channel, and the aspartic acid in position 44 (**Asp44**), which forms an indirect hydrogen bond with the NH group of the indole ring of Trp41 through a water net, at the end of the channel. Hence, meanwhile the motif HxxxW formed by H37 and W41 is the functional core of the channel, the V27 and the D44 are the gates veiling it.

The M2 is a slow channel as at physiological pH (pH=7.4) conducts at a rate of 10^2-10^3 protons per second, considered slow with respect of the constant of proton conduction through an aqueous pore of similar dimensions: 10^8 protons per second [27]. This fact is due that at physiological pH the concentration of protons is low, around one order of magnitude below the diffusion rate, however, when the external pH is lowered below the viral internal pH ($pH_{out} < pH_{in}$), this rate becomes much higher, until multiplying the diffusion rate by a second order rate constant. Hence, the conduction peak is found at low pHs [28]. This behaviour is the responsible for the sigmoidal dependence of the pH by conduction of protons through the M2 channel.

The mechanism through which the proton conduction occurs has been object of controversy in the last years [15, 29-33]. Despite this, the determination of the double dimeric structure has allowed a plausible explanation [20-21]. The protons enter the channel through the V27 gate. Once in the hydrophilic interior the protons are transported through an intermolecular translocation, thanks to the proximity of the hydrophilic residues that are facing the pore.

On a first instance the protons attach to the more N-terminal H37 and after to the more C-terminal one of the dimers which are forming an H_2 bond between the nitrogens δ i ε respectively. Following, the proton transfer
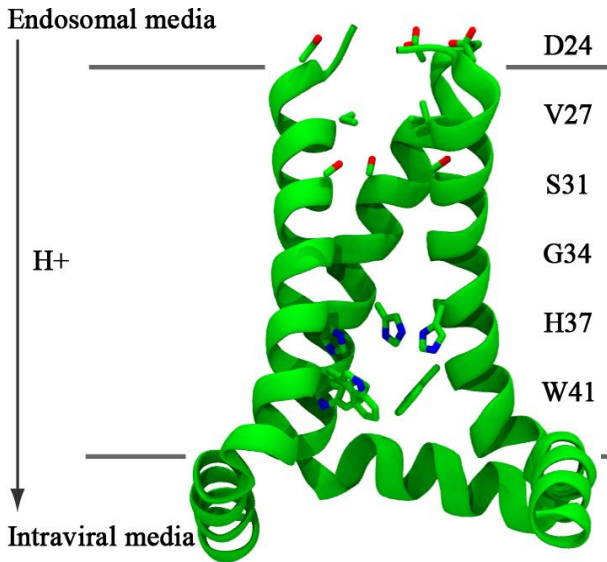
Figure 1. Schematic representation of the TM domain of the influenza A M2 channel. The side chains of the relevant residues V27, N31, H37 and W41 are shown. For clarity, only three of the four chains are shown.

from the His to the Trp occurs and the proton is then released to the viral interior. Thanks to a His37 tautomery, the protein returns to the original state. Hence, each of the dimers that form the channel is functional for the proton conduction [33]. It is important to highlight that the proximity between the H37 and the W41 – which form a stable net of cation−π interactions inside the helix and between neighbouring helixes - is the responsible of the protein tetramerization.

4. Related diseases

The influenza disease, commonly known as the flu, consists in an incubation period of two days, after which the signs and symptoms appear giving: high fever, headache, muscle and joint pain, general malaise and respiratory symptoms. Medical attention to recover from the flu for otherwise healthy patients is not usual, as symptoms normally disappear within a week. However, it can be especially aggressive giving fatal complications, among high-risk groups (children younger than two years

old, the elders and the immunosuppressed) or by a high virulent strain. Seasonal influenza outbreaks occur every year during autumn and winter in temperate regions, as there are the suitable conditions of relative humidity and temperature. Worldwide, these annual epidemics result in about 3 to 5 million cases of severe illness and about 250.000-500.000 deaths, being a clear public health treat [34]. In addition, the flu can cause serious economic losses arising from work absenteeism, productivity decrease, and saturation of health clinics during the peak illness periods [35].

However, the most important concern is the capacity of this virus to generate pandemics. These can occur through the antigenic shift, through which an especially infectious strain can combine with a highly transmissible one, giving place to a lethal unstoppable pandemic, as happened in 1918 with the Spanish Flu. The 1918 pandemic terminated with 40 million of lifes around the globe, being the most devastating of humankind history [36]. Taking this into account and knowing that those pandemics have a periodicity, the need to develop drugs to fight this virus is of vital urgency.

5. M2 channel- drug Pipeline

The M2 channel is the target of two clinically approved drugs: amantadine (Symmetrel®, Mantadix®) and rimantadine (Flumadine®).

The mechanism of action of amantadine (Amt) was object of debate in the past [37], however, nowadays it is acknowledged that only one Amt molecule binds the interior of the pore, between the residues Val27 and

Amantadine
$IC_{50}= 16.0\ \mu M$

Rimantadine
$IC_{50}= 10.8\ \mu M$
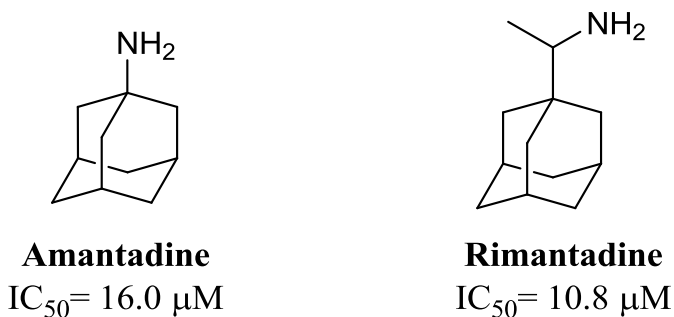
Figure 2. Commercial drugs targeting the M2 channel and corresponding IC_{50}.

Gly34 (called pore binding site), when the channel is in the open state, under acidic pH. The mechanism through which these adamantane structures inhibit the channel activity, responds to a physical blockade in which the drug occludes the pore avoiding: the proton transfer, the conformational change of the protein and the protein tetramerization.

The orientation of the polar group of the adamantane in the M2 channel had been debated as well. The two main theories were: the binding occurs in the down form [38], in which the hydrophobic cage is interacting through van der Waals forces with the methyl groups of the Val27 and Ala30, meanwhile the polar group is directed to the interior of the pore. Contrarily, in the second modality or up binding mode, the polar group is pointing the Val27 gate, being better solvated. The debate ended after proving that these two binding modes fluctuate depending on the protonation state of the M2 [39].

6. M2 as a therapeutic target

Nowadays the appearance of resistant strains together with the secondary effects in the central nervous system of Amt – known as NMDA receptor antagonist – have prompted the use of these drugs to be discouraged [40]. Surprisingly instead of causing a desertion of the M2 channel, has unchained a strong research on this protein, as it is the ideal candidate to be a drug target, presenting:

Well known biology. Nowadays the M2 channel is the best-known channel, being an ideal candidate for the rational drug design.

Essential for the viral cycle. As aforementioned, M2 channel is responsible for pH regulation in several events of the viral cycle. If the proton flow is stopped by a suitable inhibitor, the virus is no longer able to replicate.

Low mutation rate. Despite the flu virus has a high mutagenicity rate, in the case of the M2 channel, a very limited number of mutants that are both, infective and viable are known. In fact, in the circulating strains we mainly find the following 3 types [41]:

V27A (Valine ⟶ Alanine)

In this mutant channel in the position 27 the valine, which side chain is an isopropyl group, is replaced by an alanine, with a methyl group as a side chain. This destroys the entrance gate of the channel, increasing the proton conduction rate and weakening the α helix packing, which gives place to a 2 Å wider channel, respect the wild-type (*wt*). Hence, despite the inhibitors are able to bind the pore, there is not enough energetic resistance to avoid

their exit, provoking the fast drug release from the channel and restarting the proton flow. Worthy of note, the V27A is the only mutant arising from the drug selection pressure [42-43].

L26F (Leucine $\longrightarrow$ Phenylalanine)

The replacement of the leucine, with an isobutyl group, by a phenylalanine, with a benzyl group, which is placed in the interhelical interface, destabilizes the general structure of the channel. As a result, the packaging of the pore will be less compact, increasing its diameter by 0.5 Å. The widening effects are similar to those of the V27A mutation.

S31N (Serine $\longrightarrow$ Asparagine)

The S31N mutant is clinically the most relevant [44] as it is found in a 95% of the currently circulating strains. The serine (-CH$_2$OH) of the *wt* channel is replaced by an asparagine (-CH$_2$CONH$_2$) giving place to a bigger change than in the previous cases: the channel widens 0.5 Å nearby the Val27 gate and narrows on 1.5 Å in the mutation site (Asn31). In the *wt*, the Ser31 is oriented towards the membrane lipids, conformation that is not adopted in the mutant channel, as the Asn31 methylcarboxamide side chain, is longer and more hydrophilic, giving place to unfavourable interactions. This fact provokes a global restructuration of the channel that
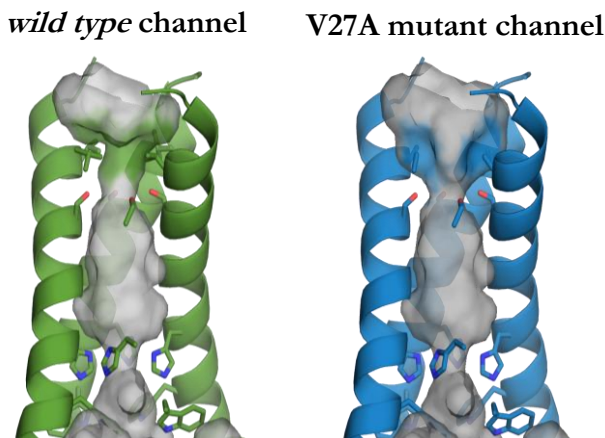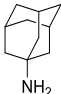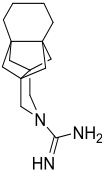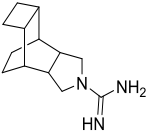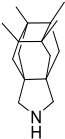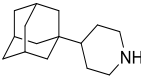

Figure 3. Schematic representation of the TM domain of the wild-type M2 channel *vs* its V27A mutant. Note the cavity expansion at the top in the V27A mutant M2 channel.

destroys the Amt binding site. In the case that Amt enters the channel, it will stablish destabilizing interactions with the Asn31 methylcarboxamide side chain, oriented towards the pore in the S31N. Despite this will justify the resistance mechanism of S31N it needs to be mentioned that the full mechanism has not yet been elucidated and there are other hypotheses [19, 45-46].

7. Our M2 oriented research line

Since the introduction of Amt in clinics in 1966 [47], hundreds of analogues have been synthesized and evaluated. In 2011, we reviewed the earlier synthetic efforts carried out before the existence of the recent functional, structural and computational studies that have provided a solid basis for structure-based drug design [48]. More recently, in 2015, Wang *et al.* updated this topic, with focus on the rationally-designed inhibitors [49].

During the past years, our group has synthesized several polycyclic Amt analogues containing different scaffolds including ring-contracted, ring-rearranged and 2,2-dialkyl derivatives of Amt. Thanks to the growing knowledge of the M2 structure and function, the rational design of new inhibitors against the resistant strains is starting to bear fruit. In the following sections we will review our own work on M2 inhibitors, with focus on four generations of inhibitors (Figure 4).
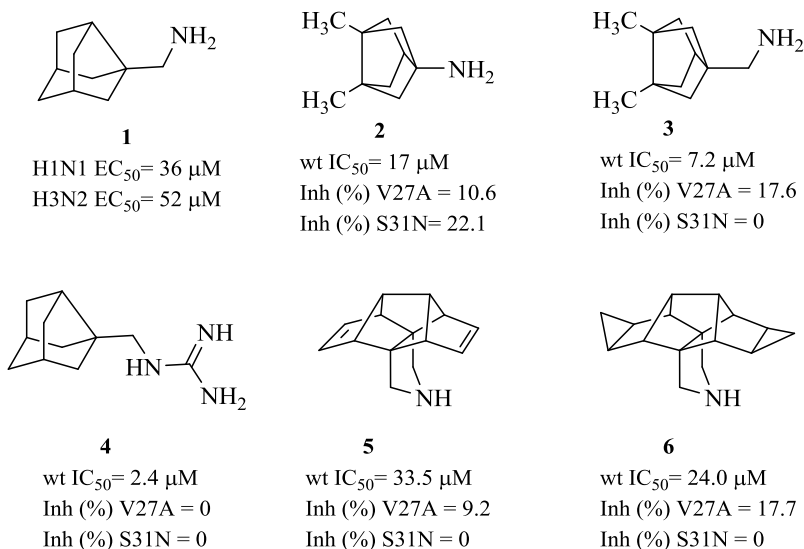

IC_{50} (μM)	Amantadine	1st generation	2nd generation	3rd generation	4th generation
wt	16	3.4	2.1	18	4.1
V27A	>100	0.3	22.6	0.7	3.6
L26F	>100	NT	NT	8.6	NT
S31N	>100	>100	>100	>100	>100
	Obsolete drug	Dual inhibitor Long synthesis	Dual inhibitor Short synthesis	Triple inhibitor New binding mode	Potency balance Insights in the mechanism of action

**Figure 4**. Summary of our M2 research line.

8. First Generation inhibitors

The first inhibitors prepared in our research group [50] steam from amine **1**, which was found to be an Influenza A compound in a wide pharmacological activity assay of Amt ring-contracted analogues prepared in the group [51]. In this early project, several ring expanded and ring contracted derivatives of Amt were synthesized and evaluated with the aim to explore the effect of modifying the inhibitor's size in the different M2 channels (at the time of unknown structure).

Resulting from this first work, several inhibitors against the *wt* channel of Influenza A virus were identified. Moreover it could be seen that the ring expanded analogues, featuring the 3-azahexacyclo[$7.6.0.0^{1,5}.0^{5,12}.0^{6,10}.0^{11,15}$] pentadecane scaffold (**5** and **6**) were able to show marginal inhibition values against the mutant V27A. More interesting was the ring contracted analogue **2**, which was able to mildly inhibit the three relevant channels of the virus [50].

1
H1N1 EC_{50}= 36 μM
H3N2 EC_{50}= 52 μM

2
wt IC_{50}= 17 μM
Inh (%) V27A = 10.6
Inh (%) S31N= 22.1

3
wt IC_{50}= 7.2 μM
Inh (%) V27A = 17.6
Inh (%) S31N = 0

4
wt IC_{50}= 2.4 μM
Inh (%) V27A = 0
Inh (%) S31N = 0

5
wt IC_{50}= 33.5 μM
Inh (%) V27A = 9.2
Inh (%) S31N = 0

6
wt IC_{50}= 24.0 μM
Inh (%) V27A = 17.7
Inh (%) S31N = 0

Figure 5. Ring contracted and ring expanded analogues prepared in a previous project. Antiviral EC_{50} values are shown for **1**. For compounds **2-6**, IC_{50} values are shown for *wt* M2 channel, while % of inhibition of the channel function by 100 μM of inhibitor for 2 min, are given for A/V27A and A/S31N mutant channels.
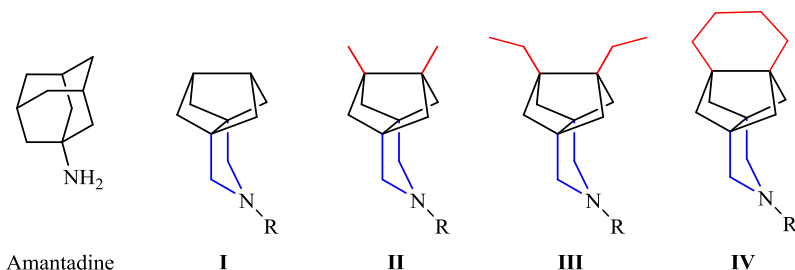
Figure 6. Analogues prepared in this project. From the bisnoradamantane scaffold (black), the length is increased in both directions with a pyrrolidine ring (blue) and with a variety of alkyl substituents (red), which confer greater length and bulkiness to the basic centre distal side.

These results promoted a further exploration of the ring contracted analogues of Amt [52]. With the aim to target the three main channels we envisaged a series of bisnoradamantane-like scaffolds, 3-azatetracyclo[5.2.1.1^{5,8}.0^{1,5}]undecanes, which were modified to be greater in length than Amt –feature that had been seen beneficial when targeting the wider V27A- but with a slight width reduction compared to this commercial drug –thought to be required to inhibit the narrower mutant S31N (Figure 6).

In addition, for this family of derivatives, the basic centre was introduced in a pyrrolidine scaffold. This modification had three main purposes: i) to increase the compound's length in the basic centre proximal site; ii) to confer a fixed orientation to this basic centre, and iii) to reduce the conformational freedom of the basic centre.

8.1. Synthetic route

We will exemplify the synthesis of compounds of general structure I-IV using the smaller analogues **16**-**18** (Scheme 2) [52]. To access dicarboxylic acid **14**, key precursor of the depicted compounds, a synthetic route previously described in the group was followed [53-54] (Scheme 1).

The synthesis started with a Weiss reaction [55-56], which implies the condensation of the α-dicarbonylic compound glyoxal with two equivalents of dimethyl 1,3-acetonedicarboxylate, in basic media. Interestingly this unique reaction consists in two aldol condensations, two dehydrations and two Michael reactions that afford the bicyclic adduct **7** in
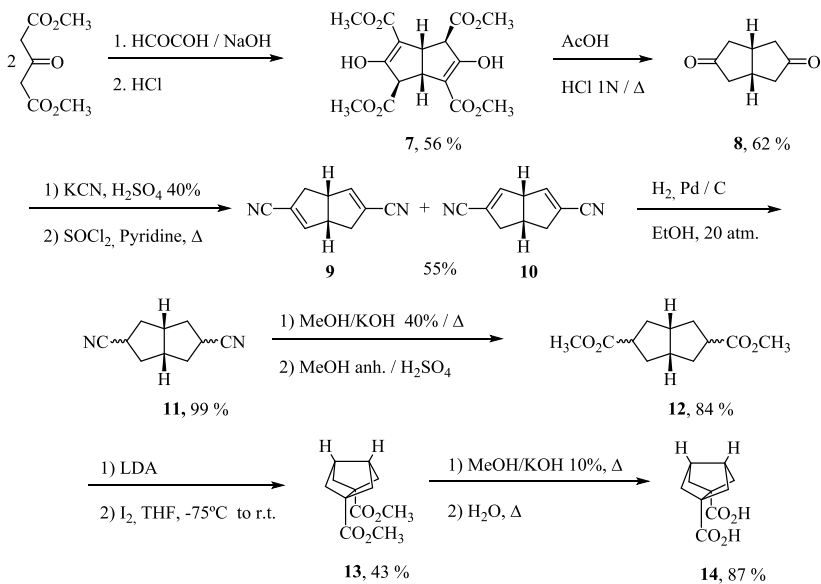
Scheme 1. Preparation of the key bisnoradamantane diacid **14**

moderate yields. The dienol-tetraester **7** is then treated with acetic and hydrochloric acids in water, undergoing a hydrolysis and decarboxylation to the symmetric diketone **8** [57]. In aqueous media with neutral pH - regulated by dropwise addition of 40% sulphuric acid - the diketone intermediate was reacted with potassium cyanide to give a stereoisomeric mixture of bis-cyanohydrines. This mixture was readily dehydrated using thionyl chloride in pyridine at reflux, to the regioisomeric mixture of dinitriles **9** and **10**. After sublimation of the mixture of **9** and **10**, in order to remove sulfur traces, a catalytic hydrogenation, using 10 % Pd/C as catalyst and 20 atm of pressure, yielded the stereoisomeric mixture **11**, composed of the three possible reduced products. Following, this mixture was hydrolysed with KOH in a methanol/water media and the bicyclic diacid obtained was immediately esterified, using Fisher's conditions, to the regiomeric ester mixture **12**. Upon reaction of **12** with the basic non-nucleophile lithium diisopropylamide (LDA), the lithium bis-enolates were coupled by a iodine-mediated oxidation. This cyclization step was key in order to build up the bisnoradamantane scaffold, immediate precursor of the target compounds.

A final hydrolysis in basic media furnished the desired bisnoradamantane diacid **14**, upon which we started the envisaged 3-step synthetic route towards our first 3-azatetraciclo[5.2.1.1^{5,8}.0^{1,5}]undecane product (Scheme 2).
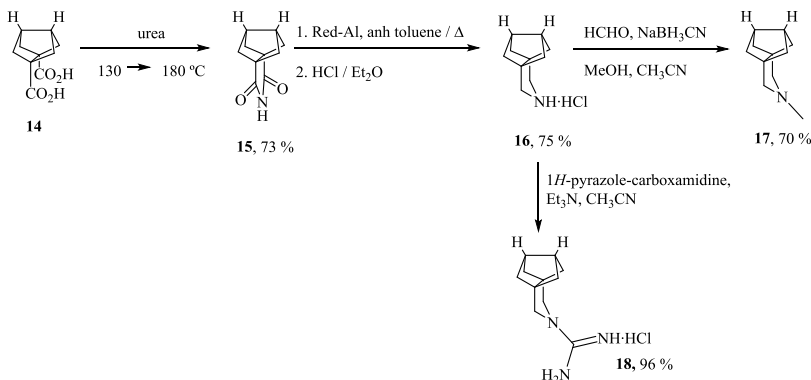
Scheme 2. Route towards compounds **16**, **17** and **18**.

The reaction of **23** with urea at 180ºC furnished the imide **15**, which was reduced using Red-Al® to **16**. From this amine **16**, the guanidine derivative **18** and the tertiary amine **17** were easily synthesized using standard procedures.

Starting from a suitably substituted diketone analog of **8**, compounds featuring scaffolds **II-IV** were accessed in an analogous way [52].

8.2. Pharmacological evaluation

After pharmacological testing, this work showed that, starting from compounds active only against the *wt* A/M2 channel, it is possible to design compounds active against both the *wt* and the V27A mutant A/M2 channels. In fact, some of them inhibit both channels more effectively than Amt inhibits the *wt*. For example, while amine **16** and guanidine **18** were only active against the *wt* A/M2 channel (IC$_{50}$ = 11.7 and 1.05 μM, respectively), the corresponding analogues derived from series **IV** were endowed with dual inhibition of the *wt* (e.g., IC$_{50}$ = 3.4 μM for the guanidine), and the V27A mutant (e.g., IC$_{50}$ = 0.3 μM for the guanidine) A/M2 channels. Of note, the low micromolar antiviral activity of the three dual inhibitors identified, amine from series **IV** and guanidines from series

II and **IV**, was confirmed by an influenza virus yield assay [52]. Interestingly, *these were the first non-adamantane compounds endowed with this dual activity reported in the literature*, opening the way to the design of novel M2 inhibitors structurally based on non-adamantane scaffolds.

9. Second and third generation inhibitors

The endeavour described herein has its origins in our previous project (see above) in which we observed that the polycyclic amines, which were greater in length but featured a reduction in the polycyclic core width in respect to amantadine, were endowed with dual activity against the *wt* and the V27A mutant channels from Influenza A virus.

With the objective of further exploring this strategy and taking into account that:

- Several structures of the M2 *wt* channel were available at the time [19, 29,58], which allowed a tailoring of our compounds to the binding site.
- The structure of the V27A mutant had been disclosed, reporting wider diameters of the pore [59].
- Our hypothesis that, in order to target the V27A mutant, greater lengths might be required. Presumably this would allow the basic centre of our molecules to establish interactions with the Gly34 in the lower binding site of the channel, disrupting the deeper water clusters and blocking the pore [60].
- Coming from a resource consuming synthetic route of 12 steps, which included challenging reactions and the use of hazardous reagents to reach the first bioactive compound, this time we aimed for ready-access compounds, this is, the new bioactive polycycles should be prepared in few synthetic steps [61].

The following three polycyclic scaffolds: 4-azatetracyclo[5.3.2.0^{2,6}.0^{8,10}] dodecanes (**V**), 4-azatetracyclo[5.4.2.0^{2,6}.0^{8,11}]tridecane (**VI**) and 7,8,9,10-tetramethyl-3-azapentacyclo[7.2.1.1^{5,8}.0^{1,5}.0^{7,10}]tridecane (**VII**), were envisaged at the start of this work (Figure 7).

These structures were meeting the sought criteria, being greater in length than our previous family of compounds and the first bioactive compound of each series was accessible in only 2 synthetic steps in the case of **V** and **VI** or 5 steps in the case of **VII**. In addition, these scaffolds offered diverse chemically modifiable points, which allowed us to prepare a family of derivatives for each series.
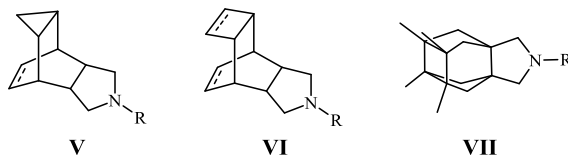
Figure 7. Designed polycycles with putative anti-influenza A activity.

9.1. Synthetic route

The **V** and **VI** families were synthesized in parallel [61]. The synthesis started with the reaction of maleimide with either cycloheptatriene (for the preparation of **V**) or cyclooctatetraene (for the preparation of **VI**) in a heated sealed tube. Interestingly, in this reaction –previously reported by Abou-Gharbia and co-workers [62], the cyclooctatetraene, **19**, under high temperatures, isomerizes to its valence isomer bicyclo[4.2.0]octa-2,4,7-triene, **20**, by means of a thermal 6e$^-$ electrocyclic pericyclic reaction [63-65]. This *in situ* formed specie is the diene that reacts with the dienophile maleimide in the subsequent Diels-Alder reaction, yielding the tetracyclic *endo*-adduct **21**.
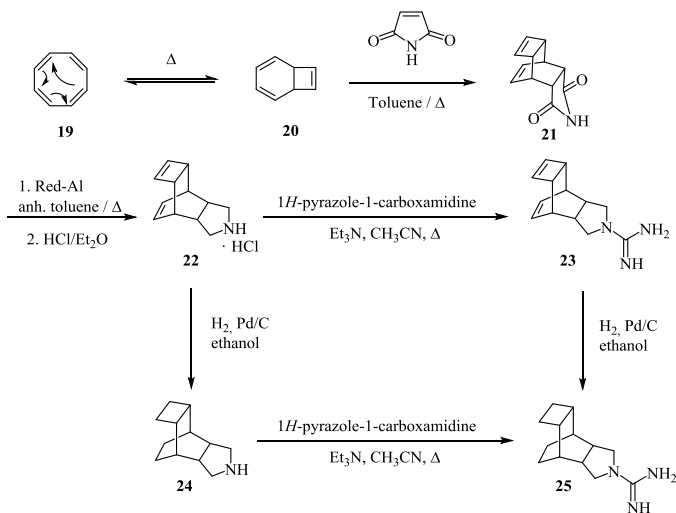
Scheme 3. Synthetic route to 4-azatetracyclo[5.4.2.0^{2,6}.0^{8,11}]tridecane derivatives with antiviral activity. The ring-contracted analogues derived from **V** were synthesized using the same synthetic route but starting from cycloheptatriene [61].

A double reduction of the imide **21** carbonyl groups using Red-Al®, lead to the first bioactive product, the pyrrolidine **22**. From this key intermediate **22** the desired saturated derivative, **24**, and their corresponding guanidines, **23** and **25**, were easily accessed through an hydrogenation with Pd/C as catalyst and a reaction with 1*H*-pyrazole-1-carboxamidine, respectively.
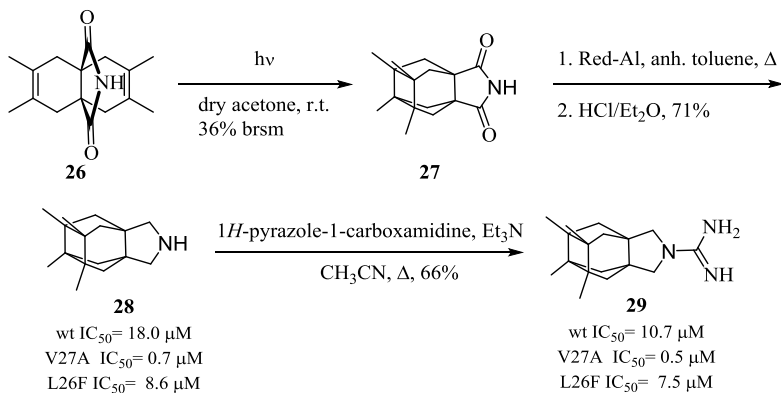
Scheme 4. Synthesis of the third generation: **28** and **29**, triple inhibitors of the *wt*, V27A and L26F mutant channels of influenza A [61].

We were aiming to improve our previous results and, for this, in our third generation we designed a structurally unrelated scaffold which was wider and longer in respect to amantadine's structure. Following this idea the family **VII** was prepared. Starting from the known imide **26**, this molecule gave access to the new pentacyclic core in only one step, which involved a [2+2] photocycloaddition under UV light. Even the 36% yield of this step was relatively low, the rapid access to the desired **VII** scaffold shift the balance positively towards this synthetic strategy. Upon isolation of imide **26**, the usual synthetic path yielded amine **28** and guanidine **29**.

9.2. Pharmacological evaluation

The inhibitory activity of the compounds was tested on A/M2 channels expressed in *Xenopus* oocytes using the two-electrode voltage clamp (TEVC) technique. Regarding the second-generation compounds (scaffolds

V and **VI** in Figure 7), the four derivatives of scaffold **VI** (amines **22** and **24** and guanidines **23** and **25**) and their corresponding analogues derived from scaffold **V** were low micromolar inhibitors of the *wt* channel (e.g., IC_{50} = 16.0 and 1.2 μM for Amt and **24**, respectively). Regarding the activity against the V27A M2 mutant channel, three trends were found, i.e., guanidine performed better than its corresponding amine, the fully saturated compounds were more potent than their corresponding unsaturated analogues, and the derivatives of **V** were less potent than the ring-expanded derivatives of **VI**. Not unexpectedly, the larger compound from this series, guanidine **25**, was the more promising compound, being more potent than Amt against the *wt* M2 channel (IC_{50} = 2.1 μM) and endowed with fair activity against the V27A mutant channel (IC_{50} = 22.6 μM). Overall, this second generation compounds led to dual inhibitors in very short synthetic routes [61].

The next challenge, to be able to target more mutant channels while keeping very short synthetic sequences, was achieved with the third generation of inhibitors (scaffold **VII**, Figure 7 and Scheme 4). Strikingly, we could report, for the first time in the literature, potent triple inhibitors lacking the adamantane scaffold. Thus, our new compounds **28** and **29** were able to potently inhibit at once three different M2 channels: the *wt* and the mutants V27A and L26F. On the top of that, **28** and **29** were equipotent to amantadine for the *wt* and clear superior inhibitors of the V27A and the L26F mutant.

In addition, this unforeseen activity prompted an in-depth study of **28** binding mode by Prof. F. J. Luque and co-workers. Through molecular dynamics simulations, a clear difference between the binding of this amine **28** in the *wt* or in the V27A mutant channel could be spotted. Meanwhile in the *wt* the binding occurred with the basic group pointing towards the viral interior –the so called *down* binding mode- paralleling the one that Amt displays; in the case of the V27A this compound is found in equilibria between the *down binding mode* and the *up binding mode* – where the basic moiety points towards the viral exterior. The key feature for this compound to be stabilized in the *up binding mode*, preventing its rapid release to the cytoplasm, was found to be the four methyl substituents placed in the upper part of the molecule [61].

The presented families show the feasibility of designing easily accessible compounds able to successfully inhibit the *wt* and the V27A and L26F variants of the A/M2 channels of influenza A virus. In fact, some of the newly designed compounds inhibit the three channels similarly or even
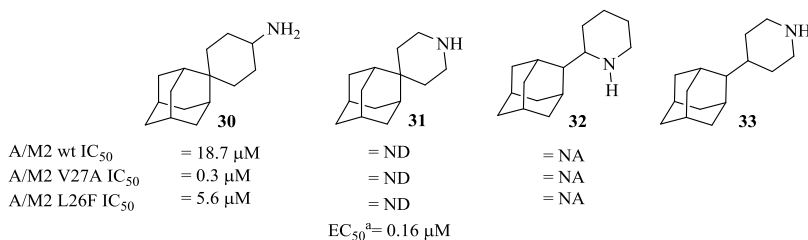
more effectively than Amt inhibits the *wt* proton channel. In particular, amine **28** and guanidine **29** emerged as promising compounds, being low micromolar inhibitors against the *wt* channel and the L26F mutant, while being endowed with submicromolar IC_{50} against the V27A variant. Furthermore, compound **28** showed strong activity against the A/PR/8/34 strain, an A/H1N1 virus with two mutations (S31N and V27T) in the M2 protein. However, taking into account that this compound was devoid of activity against the S31N M2 mutant channel, this activity must be related with an alternative mechanism of action, as we and others have comprehensively discussed [66-67]. Overall, these results suggest that compounds **28** and **29** are suitable templates to explore novel candidates against influenza virus.
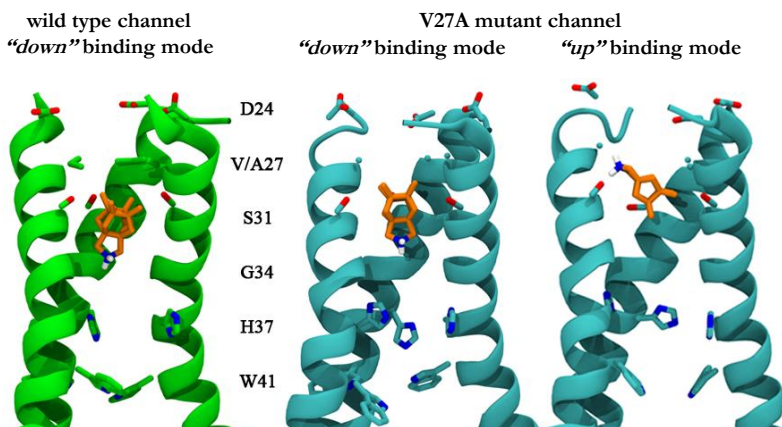
Figure 8. Amine **28** bound to the *wt* ("down" bonding mode) and the V27A mutant channels ("down" and "up" binding modes). For clarity, only 3 chains are shown.

10. Fourth generation inhibitors

Regardless our previous efforts in the anti-influenza research line had been mainly oriented to replace the adamantane scaffold by a more suitable polycycle [50,52,61], the disclosure of several M2 channel structures with bound amantadine [19,58,68] or adamantane containing compounds [69], provided new detailed insights of the binding mode of adamantane-like molecules. Hence, we decided to take advantage of this recent knowledge to, building up on our expertise, design adamantane related compounds with improved features to display an upgraded inhibition profile.

A/M2 wt IC$_{50}$	= 18.7 μM	= ND	= NA
A/M2 V27A IC$_{50}$	= 0.3 μM	= ND	= NA
A/M2 L26F IC$_{50}$	= 5.6 μM	= ND	= NA
		EC$_{50}$[a] = 0.16 μM	

Figure 9. Anti-influenza adamantyl compounds: spiro compound **30**, piperidines **31** and **32** and the novel envisaged analogue **33**. [a]EC$_{50}$ determined in the influenza A/HongKong/7/87/H3N2 strain, which carries a *wt* channel.

In line with this, DeGrado's group disclosed in 2011 the spiro compound **30**, which shows an outstanding activity against the V27A, the L26F mutant and the *wt* M2 channels [70]. Worthy of note, Kolocouris *et al.* had previously reported the synthesis of **32**, an adamantyl piperidine related to **30** [71], which failed to show activity against an Influenza strain carrying an Amt-resistant S31N mutant M2 channel (A/X31, H3N2), and its isomeric piperidine **31** [72-73] that was found to be active against an strain containing a *wt* M2 channel (A/HongKong/7/87/H3N2). They also showed that the lowest energy conformation of **32**, resulted in a geometry quite different that the one shown by the amines **30** and **31**. These facts made us question the importance of the basic centre position in the molecule; hence, in our new designs we orientated this polar group towards the terminal histidines and perpendicular to the protein backbone, analogously to **30** (Figure 9).

To further address the basic centre orientation remark, besides modifying the position of the nitrogen atom in the piperidine ring, we decided to investigate which was the most suitable anchoring point for this ring, in the adamantane scaffold. For this we prepared two series of adamantyl piperidine analogues bearing the heterocycle in the adamantane C1 (as in amantadine) or C2 (as in the triple inhibitor **30**) positions [74]. Our designs were first studied *in silico* by Luque's group. Their theoretical calculations indicated that our compounds were very similar to **30**, so their increased length with respect to Amt could provide an improvement of the inhibitory activity.

In light of those predictions we decided to prepare an extra series of C-2 analogues featuring a methylene group between the lipophilic core and the ring, displaying even longer scaffolds.

10.1. Synthesis

First we undertook the synthesis of the C-1 series. Paralleling the work of Togo and coworkers [75], the isomeric mixture of the pyridine derivatives **44** and **45** was readily obtained after the radical decarboxylation of the carboxylic acid **43** in the presence of pyridine. In this reaction the first step is the acid-base exchange between the 1-adamantane carboxylic acid and the pyridine. Next, the [bis(trifluoroacetoxy)iodo]benzene reacts with the *in situ* generated adamantane carboxylate, displacing the trifluoroacetate moieties, to give [bis(1-adamantanecarboxyl)iodo]benzene. This species undergoes a radical decarboxylation to generate an adamantly radical, which adds to the pyridinium cation that finally, rearomatizes to yield the desired addition products **35** and **36**.

After a simple chromatography separation of both isomers, a catalytic hydrogenation with platinum oxide (IV) as catalyst, yielded the desired piperidines **37** and **38**. The usual guanidine derivative was build up for **37**, in a 76% yield. Despite our several attempts, the analogous reaction over the piperidine **38** was repeatedly unsuccessful, presumably reflecting the greater steric congestion around this nitrogen atom (Scheme 5).
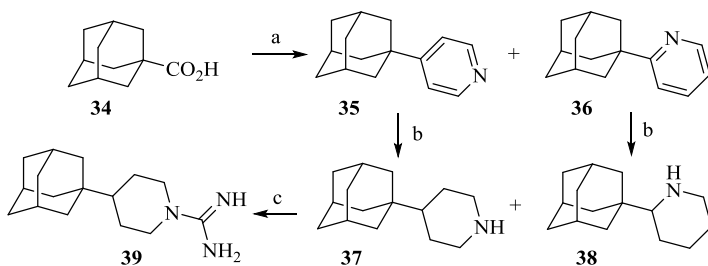
Scheme 5. Synthesis of 4-(1-adamantyl)piperidines. *ᵃ*Reagents and conditions: a: pyridine, [bis(trifluoroacetoxy)iodo]benzene, anh. benzene, reflux, overnight, **35**, 9%; **36**, 27%; b: H₂, PtO₂, MeOH, 30 atm, 97% yield for **37**; 99% yield for **38**; c: 1*H*-pyrazole-1-carboxamide hydrochloride, anh. Et₃N, acetonitrile, reflux, 6 h, 76% yield.
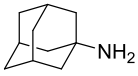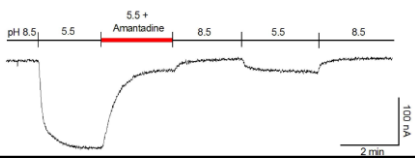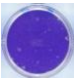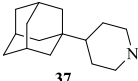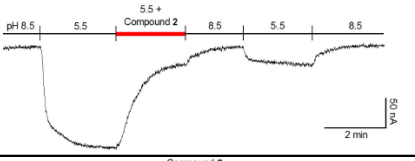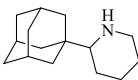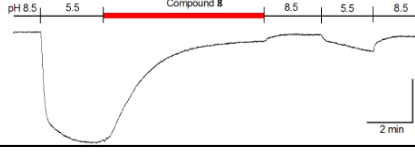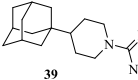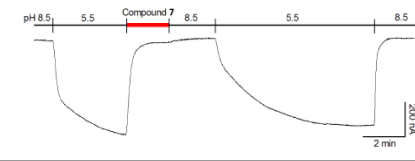
After this, the compounds belonging to the C-2 series were prepared (Scheme 6). The preparation of both series was envisaged through the same synthetic sequence starting with the addition to 2-adamantanone of the corresponding *in situ* generated organolithium reagent, 4-pyridil lithium or 4-picolinyl lithium, respectively. The formed adamantyl pyridine species

was then hydrogenated using platinum oxide as catalyst, to give the first bioactive compound (**33** and **46**). The tertiary alcohol group of **46** was eliminated to yield olefin **47** that was further hydrogenated using 10% palladium over active charcoal as catalyst to give the saturated analogue **48**. The saturated compounds, **33** and **48** were converted to tertiary amines through a reductive alkylation reaction with acetaldehyde or formaldehyde, to furnish **44** and **49**, respectively. Finally, amines **47** and **48** reacted with 1*H*-pyrazole-1-carboxamidine hydrochloride furnishing the guanidine derivatives **50** and **51**, respectively [74].
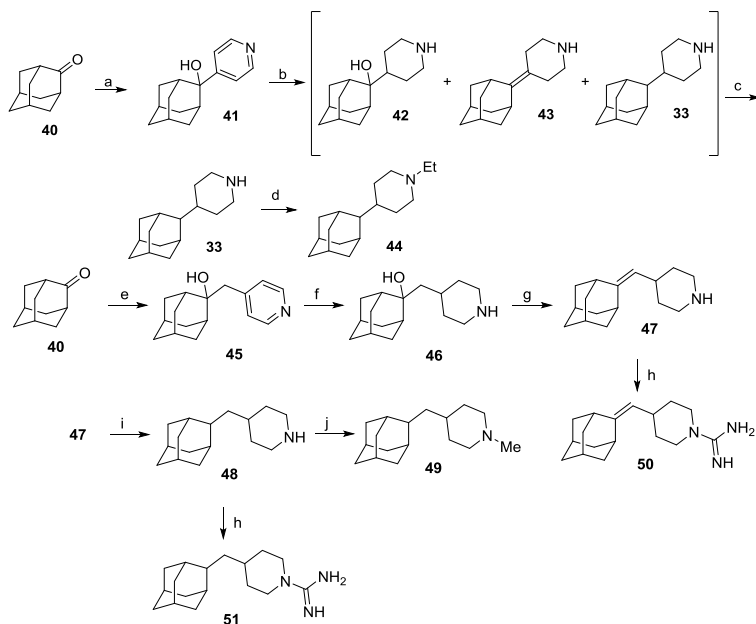
Scheme 6. Synthetic route for the preparation of the adamantyl piperidine C-2 series**.** Reagents and conditions: **a**: 4-pyridyl lithium; Et$_2$O/THF, -65 °C to rt, 70% yield; **b**: 1 atm H$_2$, PtO$_2$, ethanol, rt, 24 h, 93% yield of a mixture of **42**, **43** and **33**; **c**: 1) SOCl$_2$, pyridine, anh. CH$_2$Cl$_2$, -60 °C, 30 min, 2) 1 atm H$_2$, Pd/C, methanol, HCl, rt, 2 h, 63% overall yield; **d**: acetaldehyde, NaCNBH$_3$, AcOH, methanol, rt, 24 h, 76% yield; **e**: 4-picoline, anh THF, *n*-BuLi, 2 h, rt, 90% yield; **f**: 1 atm H$_2$, PtO$_2$, HCl, methanol, 5 days, > 99% yield; **g**: SOCl$_2$, pyridine, anh. CH$_2$Cl$_2$, -60 °C, 30 min, > 99% yield; **h**: 1*H*-pyrazole-1-carboxamidine hydrochloride, anh Et$_3$N, acetonitrile, 70 °C, 6 h, 88% yield for **50**, 64% yield for **51**; **i:** 1 atm H$_2$, Pd/C, methanol, HCl, rt, 2 h, 68% yield; **j**: formaldehyde (37% aqueous solution), NaCNBH$_3$, AcOH, rt, 18 h, 73% yield.

Table 1. Pharmacological assays in M2/*wt* wrap up. [a]Isochronic (2 min) values for IC_{50} are given. [b]TEVC technique in *Xenopus* oocytes. [c]EC_{50} based on 72-h compound exposure time.

Influenza A *wt*	IC_{50} μM [a]	Kinetics[b]	EC_{50} μM [c]
Amt	16.0		0.2
37	4.1		0.2
38	ND		0.8
39	1.9		>50
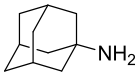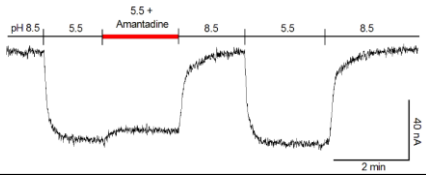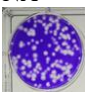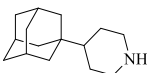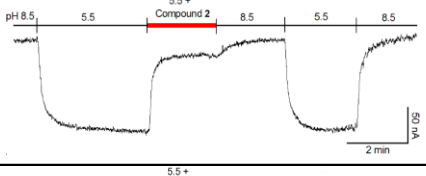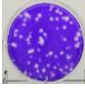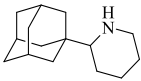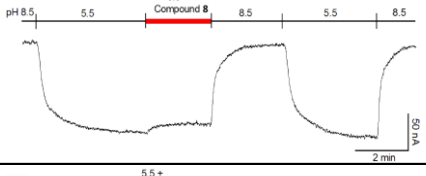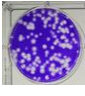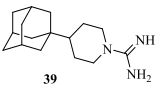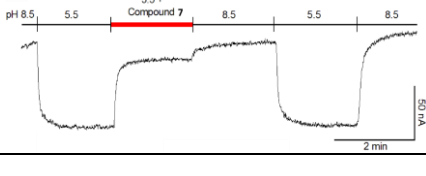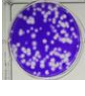
10.2. Pharmacological evaluation

As in previous series, the antiviral activities and the channel blocking abilities of the new compounds were measured; this time, however, further TEVC assays, to assess the kinetics of the M2 channel inhibitors were carried out (Table 1 and Table 2) [74]. From these results a lack of correlation was observed between those coming from the isochronic inhibition assays, in which several compounds displayed potent M2 blockade (both on the *wt* and the V27A M2 mutant channel), and the antiviral activity assays, in which a reduced number of our molecules were identified as antivirals. Steaming from these observations we could

experimentally prove the V27A resistance mechanism previously proposed *in silico* and through NMR studies.

In table 1 it can be seen that only the compounds with slow K_{off} (as Amt, **37** and **38**) display antiviral activity, regardless their channel blocking ability. The importance of slowly leaving the channel before the rate of binding to it, can be seen when comparing **39**, which displays M2 blockade at 2 min but not antiviral activity, and **38**, that does not block the channel upon short exposure, due to a slow K_{on}, but displays antiviral activity (because of slow K_{off}).

Table 2. Pharmacological assays in M2/V27A wrap up. [a]Isochronic (2 min) values for IC_{50} are given. [b]TEVC technique in *Xenopus* oocytes. [c]EC_{50} based on 72-h compound exposure time. NA = Not active. ND = EC_{50} not determined.

Influenza A V27A	IC_{50} μM [a]	Kinetics[b]	EC_{50} μM [c]
Amt	> 500		NA
37	3.6		ND
38	> 500		NA
39	16.2		NA

The main evidence for the mechanism of resistance of the V27A mutant M2 channel is the behaviour of amine **37**. This compound is able to block both the *wt* (IC$_{50}$ = 4.1 μM) and the V27A mutant (IC$_{50}$ = 3.6 μM) M2 channels in the typical TEVC experiments (2 min). However, for the V27A mutant, the block is only maintained for a short time, because weak binding affinity facilitates dissociation during washing with drug-free pH 8.5 buffer, after which the blocker is released from the channel that becomes functional again. This fact explains why **37** is active as antiviral against a strain carrying the *wt* channel but lacks activity against a strain carrying the V27A mutant M2 channel (compare Table 1 and 2) [74]. Our new experimental evidence for V27A drug resistance reinforces the previous computational [76-80] and structural [59] hypothesis and may lead to a more profound comprehension on how Influenza A virus acquires resistance, to eventually shed light to drug design.

11. Conclusion

Overall our research has allowed to move from Amt, inactive against the three main mutants, to potent dual inhibitors with a complex synthesis (first generation) which was later on simplified reaching potent dual inhibitors in only two synthetic steps (second generation). Following the most potent triple inhibitor at the time, was accessed in few synthetic steps and featuring an unforeseen polycyclic scaffold (third generation). Finally with the fourth generation the *in silico* predicted drug resistance mechanism of the V27A mutant channel, could be demonstrated.

We hope that all these findings, along with the recent paramount advances on the understanding of the proton conductance mechanisms [81-85] and mutant M2 channels structure [86-87] will bring the antiinfluenza A drug research closer to the discovery of a suitable drug to fight the virus [88-93].

Finally is worth mentioning the combined antiviral therapy has raised great interest as a strategy to fight the influenza virus [94-95]. Similar to the antiretroviral therapy, this will consist in the administration of a drug cocktail that will target different steps of the viral cycle. We believe that the drugs targeting the viral protein HA will be excellent allies to the M2 blockers for this purpose [96].

Acknowledgements

References

1. Ghedin, E., Sengamalay, N. A., Shumway, M., Zaborsky, J., Feldblyum, T., Subbu, V., Spiro, D. J., Sitz, J., Koo, H., Bolotov, P., Dernovoy, D., Tatusova, T., Bao, Y., St George, K., Taylor, J., Lipman, D. J., Fraser, C. M., Taubenberger, J. K., Salzberg, S. L. Large-scale sequencing of human influenza reveals the dynamic nature of viral genome evolution. 2005, *Nature*, 437, 1162.
2. WHO. Bull. A revision of the system of nomenclature for influenza viruses: a WHO Memorandum. 1980, *World Health Organ*., 58, 585.
3. Centers for Disease Control and Prevention: http://www.cdc.gov/flu/about/viruses/change.htm (10 Jun 2017).
4. Bouvier, N. M., Palese, P. The biology of influenza viruses. 2008, *Vaccine*, 26, D49.
5. Skehel, J. J., Wiley, D. C. Receptor binding and membrane fusion in virus entry: the influenza hemagglutinin. 2000, *Annu. Rev. Biochem.*, 69, 531.
6. de Vries, E., Tscherne, D. M., Wienholts, M. J., Cobos-Jiménez, V., Scholte, F., García Sastre, A., Rottier, P. J. M., de Haan, C. A. M. Dissection of the influenza a virus endocytic routes reveals macropinocytosis as an alternative entry pathway. 2011, *PLoS Pathog*., 7, e1001329.
7. Lin, X., Noel, J. K., Wang, Q., Ma, J., Onuchic, J. N. Lowered pH Leads to Fusion Peptide Release and a Highly Dynamic Intermediate of Influenza Hemagglutinin. 2016, *J. Phys. Chem. B.*, 5, 6775.
8. Carr, C. M., Kim, P. S. A spring-loaded mechanism for the conformational change of influenza hemagglutinin. 1993, *Cell*, 73, 823.
9. Samji, T. Influenza A: Understanding the viral life cycle. 2009, *Yale J. Biol. Med.*, 82, 153.
10. Krug, R. M. Functions of the influenza A virus NS1 protein in antiviral defense. 2015, *Curr. Opin. Virol.* 12, 1.
11. Takeuchi, K., Lamb, R. A. Influenza virus M2 protein ion channel activity stabilizes the native form of fowl plague virus hemagglutinin during intracellular transport. 1994, *J. Virol*., 68, 911.
12. Schmidt, N. W., Mishra, A., Wang, J., DeGrado, W.F., Wong, G. C. Influenza virus A M2 protein generates negative Gaussian membrane curvature necessary for budding and scission. 2013, *J. Am. Chem. Soc*., 135, 13710.

13. Palese, P., Tobita, K., Ueda, M., Compans, R. W. Characterization of temperature sensitive influenza virus mutants defective in neuraminidase. 1974, *Virology*, 61, 397.

14. Das, K., Aramini, J.M., Ma, L., Krug, R. M., Arnold, E. Structures of influenza A proteins and insights into antiviral drug targets. 2010, *Nat. Str. Mol. Bio*., 17, 530.

15. Wang, J., Qiu, J. X., Soto, C., DeGrado, W. F. Structural and dynamic mechanisms for the function and inhibition of the M2 proton channel from influenza A virus. 2011, *Curr. Opin. Struct. Biol*., 21, 68.

16. Wang, J., Kim, S., Kovacs, F., Cross, T. A. Structure of the transmembrane region of the M2 protein H(+) channel. 2001, *Protein Sci*., 10, 2241.

17. Martin, K., Heleniust, A. Nuclear transport of influenza virus ribonucleoproteins: The viral matrix protein (M1) promotes export and inhibits import. 1991, *Cell*, 67, 117.

18. Schnell, J. R., Chou, J. J. Structure and mechanism of the M2 proton channel of influenza A virus. 2008, *Nature*, 451, 591.

19. Stouffer, A. L., Acharya, R., Salom, D., Levine, A. S., Di Costanzo, L., Soto, C. S., Tereshko, V., Nanda, V., Stayrook, S., DeGrado, W. F. Structural basis for the function and inhibition of an influenza virus proton channel. 2008, *Nature*, 451, 596.

20. Kawano, K., Yano, Y., Matsuzaki, K. A dimer is the minimal proton-conducting unit of the influenza a virus M2 channel. 2014, *J. Molec. Bio.*, 426, 2679.

21. Andreas, L. B., Reese, M., Eddy, M. T., Gelev, V., Ni, Q. Z., Miller, E. A., Emsley, L., Pintacuda, G., Chou, J., Griffin, R. G. Structure and Mechanism of the Influenza A M218-60 Dimer of Dimers. 2015, *J. Am. Chem. Soc.*, 137, 14877.

22. Helenius, A. Unpacking the incoming influenza virus. 1992, *Cell*, 69, 577.

23. Sakaguchi, T., Leser, G. P., Lamb, R. A. The ion channel activity of the influenza virus M2 protein affects transport through the Golgi apparatus. 1996, *J. Cell. Biol*., 133, 733.

24. Hu, F., Schmidt-Rohr, K., Hong, M. NMR Detection of pH-Dependent Histidine–Water Proton Exchange Reveals the Conduction Mechanism of a Transmembrane Proton Channel. 2012, *J. Am. Chem. Soc*., 134, 3703.

25. Hu, J., Fu, R., Nishimura, K., Zhang, L., Zhou, H. X., Busath, D. D., Vijayvergiya, V., Cross, T. A. Histidines, heart of the hydrogen ion channel from influenza A virus: toward an understanding of conductance and proton selectivity. 2006, *Proc. Natl. Acad. Sci. USA*, 103, 6865.

26. Tang, Y., Zaitseva, F., Lamb, R. A., Pinto, L. H. The gate of the influenza virus M2 proton channel is formed by a single tryptophan residue. 2002, *J. Biol. Chem*., 277, 39880.

27. Decoursey, T. E. Voltage-gated proton channels and other proton transfer pathways. 2003, *Physiol. Rev.*, 83, 475.

28. Ma, C., Polishchuk, A. L., Ohigashi, Y., Stouffer, A. L., Schon, A., Magavern, E., Jing, X., Lear, J.D., Freire, E., DeGrado, W. F., Lamb, R. A. Identification of the

functional core of the influenza A virus A/M2 proton-selective ion channel. 2009, *Proc. Natl. Acad. Sci. USA*, 106, 12283.

29. Acharya, R., Carnevale, V., Fiorin, G., Levine, B. G., Polishchuk, A. L., Balannik, V., Samish, I., Lamb, R. A., Pinto, L. H., DeGrado, W. F., Klein, M. L. Structure and mechanism of proton transport through the transmembrane tetrameric M2 protein bundle of the influenza A virus. 2010, *Proc. Natl. Acad. Sci. USA.*, 107, 15075.

30. Phongphanphanee, S., Rungrotmongkol, T., Yoshida, N. Proton Transport through the Influenza A M2 Channel: Three-Dimensional Reference Interaction Site Model Study. 2010, *J. Am. Chem. Soc.*, 9, 9782–9788

31. Ivanovic, T., Rozendaal, R., Floyd, D. L., Popovic, M., Van Oijen, A. M., Harrison, S. C. Kinetics of Proton Transport into Influenza Virions by the Viral M2 Channel. 2012, *PLos One*, 7, e31566, 1-9.

32. Okada, A., Miura, T., Takeuchi, H. Protonation of histidine and histidine-tryptophan interaction in the activation of the M2 ion channel from influenza a virus. 2001, *Biochemistry*, 40, 6053-60.

33. Carnevale, V., Fiorin, G., Levine, B. G., DeGrado, W. F., Klein, M. L. Multiple Proton Confinement in the M2 Channel from the Influenza A Virus. 2010, *J. Phys. Chem. C*, 114, 20856.

34. http://www.who.int/mediacentre/factsheets/fs211/en/ (26 May 2017).

35. Molinari, N. A. M., Ortega-Sanchez, I. R., Messonnier, M. L., Thompson, W. W., Wortley, P. M.,Weintraub, E., Bridges, C. B. The annual impact of seasonal influenza in the US: measuring disease burden and costs. 2007, *Vaccine*, 25, 5086.

36. Taubenberger, J. K., Morens, D.M. 1918 Influenza: the Mother of All Pandemics. Centers for Disease Control and Prevention. 2006.

37. Kozakov, D., Chuang, G., Beglov, D., Vajda, S. Where does amantadine bind to the influenza virus M2 proton channel? 2010, *Trends Biochem. Sci.*, 35, 471.

38. Cady, S. D., Wang, J., Wu, Y., DeGrado, W. F., Hong, M. Specific Binding of Adamantane Drugs and Direction of Their Polar Amines in the Pore of the Influenza M2 Transmembrane Domain in Lipid Bilayers and Dodecylphosphocholine Micelles Determined by NMR Spectroscopy. 2011, *J. Am. Chem. Soc.*, 2, 4274.

39. Khurana, E., Devane, R. H., Dal Peraro, M., Klein, M. L. Computational study of drug binding to the membrane-bound tetrameric M2 peptide bundle from influenza A virus. 2011, *Biochim. Biophys. Acta.*, 1808, 530.

40. Hubsher, G., Haider, M., Okun, M. S. Amantadine: the journey from fighting flu to treating Parkinson disease. 2012, *Neurology*, 78, 1096.

41. Leonov, H., Astrahan, P., Krugliak, M., Arkin, I. T. How Do Aminoadamantanes Block the Influenza M2 Channel, and How Does Resistance Develop? 2011, *J. Am. Chem. Soc.*, 133, 9903.

42. Furuse, Y., Suzuki, A., Kamigaki, T., Oshitani, H. Evolution of the M gene of the influenza A virus in different host species: large-scale sequence analysis. 2009, *J. Virol.*, 6, 67.

43. Furuse, Y., Suzuki, A., Oshitani, H. Large-scale sequence analysis of M gene of influenza A viruses from different species: Mechanisms for emergence and spread of amantadine resistance. 2009, *Antimicrob. Agents Chemother*., 53, 4457.

44. Dong, G., Peng, C., Luo, J., Wang, C., Han, L., Wu, B., Ji, G., He, H. Adamantane-resistant influenza A viruses in the world (1902-2013): frequency and distribution of M2 gene mutations. 2015, *PLoS One*., 10, e0119115.

45. Pielak, R. M., Oxenoid, K., Chou, J. J. Structural investigation of rimantadine inhibition of the AM2-BM2 chimera channel of influenza viruses. 2011, *Structure*, 19, 1655.

46. Can, T. V., Sharma, M., Hung, I., Gor'kov, P. L., Brey, W. W., Cross, T. A. Magic Angle Spinning and Oriented Sample Solid-State NMR Structural Restraints Combine for Influenza A M2 Protein Functional Insights. 2012, *J. Am. Chem. Soc.*, 134, 9022.

47. Hay, A. J., Wolstenholme, A. J., Skehel, J. J., Smith, M. H. 1985, *EMBO J.*, 4, 3021.

48. Duque, M. D.; Valverde, E.; Barniol, M.; Guardiola, S.; Rey, M.; Vázquez, S. Inhibitors of the M2 channel of the influenza A virus. In Recent Advances in Pharmaceutical Sciences; Muñoz-Torrero, D., Ed.; Transworld Research Network: Kerala, India, 2011; pp 35−64.

49. Wang, J.; Li, F.; Ma, C. Recent progress in designing inhibitors that target the drug resistant M2 proton channels from the influenza A viruses. 2015, *Biopolymers*, 104, 91.

50. Duque, M. D., Ma, C., Torres, E., Wang, J., Naesens, L., Juárez-Jiménez, J., Camps, P., Luque, F. J., DeGrado, W. F., Lamb, R. A., Pinto, L. H., Vázquez, S. Exploring the size limit of templates for inhibitors of the M2 ion channel of influenza A virus. 2011, *J. Med. Chem.*, 54, 2646.

51. Camps, P., Duque, M. D., Vázquez, S., Naesens, L., Clercq, E. De, Sureda, F. X., López-Querol, M., Camins, A., Pallàs, M., Prathalingam, S. R., Kelly, J. M., Romero, V., Ivorra, M. D., Cortés, D. Synthesis and pharmacological evaluation of several ring-contracted amantadine analogs. 2008, *Bioorg. Med. Chem.*, 16, 9925.

52. Rey-Carrizo, M., Torres, E., Ma, C., Barniol-Xicota, M., Wang, J., Wu, Y., Naesens, L., DeGrado, W.F., Lamb, R. A., Pinto, L. H., S. Vázquez. 3-Azatetracyclo $[5.2.1.1^{5,8}.0^{1,5}]$undecane derivatives: from wild-type inhibitors of the M2 ion channel of influenza A virus to derivatives with potent activity against the V27A mutant. 2013, *J. Med. Chem*., 56, 9265.

53. Camps, P., Iglesias, C., Rodríguez, M. J., Grancha, M. D., Gregori, M. E., Lozano, R., Miranda, M. A., Figueredo, M., Linares, A. A short synthesis of dimethyl tricyclo$[3.3.0.0^{3,7}]$octane-1,5-dicarboxylate and its 3,7-dimethyl derivative. A new route to the tricyclo$[3.3.0.0^{3,7}]$octane skeleton. 1988, *Chem. Ber*., 121, 647.

54. Camps, P., Font-Bardia, M., Pérez, F., Solans, X., Vázquez, S. Synthesis, Chemical Trapping, and Dimerization of 3,7-Dimethyltricyclo$[3.3.0.0^{3,7}]$oct-

1(5)-ene: [2+2] Retrocycloaddition of the Cyclobutane Dimer. 1995, *Angew. Chem., Int. Ed. Engl*., 34, 912.

55. Fu, X., Cook, J. M. 1992, *Aldrichimica Acta*., 25, 43.

56. Gupta, A. K., Fu, X., Snyder, J. P., Cook, J. M. General approach for the synthesis of polyquinenes via the Weiss reaction. 1991, *Tetrahedron*, 47, 3665.

57. Bertz, S. H., Cook, J. M., Gawish, A., Weiss, U. *Org. Synth. Coll. Vol. VII*, Wiley: New York, 1990, 50.

58. Cady, S. D., Schmidt-Rohr, K., Wang, J., Soto, C. S., DeGrado, W. F., Hong, M. Structure of the amantadine binding site of influenza M2 proton channels in lipid bilayers. 2010, *Nature*, 463, 689.

59. Pielak, R. M., Chou, J. J. Solution NMR structure of the V27A drug resistant mutant of influenza A M2 channel. 2010, *Biochem. Biophys. Res. Commun*., 401, 58.

60. Hong, M., DeGrado, W. F. Structural basis for proton conduction and inhibition by the influenza M2 protein. 2012, *Protein Sci*., 21, 1620.

61. Rey-Carrizo, M., Barniol-Xicota, M., Ma, C., Frigolé-Vivas, M., Torres, E., Naesens, L., Llabrés, S., Juárez-Jiménez, J., Luque, F. J., DeGrado, W. F., Lamb, R. A., Pinto, L. H., Vázquez, S. Easily accessible polycyclic amines that inhibit the wild-type and amantadine-resistant mutants of the M2 channel of influenza A virus. 2014, *J Med Chem*., 57, 5738.

62. Abou-Gharbia, M., Patel, U. R., Webb, M. B., Moyer, J. A., Andree, T. H., Muth, E. A. Polycyclic aryl- and heteroarylpiperazinyl imides as 5-HT1A receptor ligands and potential anxiolytic agents: synthesis and structure-activity relationship studies. 1988, *J. Med. Chem.*, 31, 1382.

63. Huisgen, R., Mietzsch, F. The Valence Tautomerism of Cyclooctatetraene. 1964, *Angew. Chem., Intl. Ed. Engl.*, 3, 83.

64. Vogel, E., Kiefer, H., Roth, W. R. Bicyclo[4.2.0]octa-2,4,7-triene. 1964, *Angew. Chem., Intl. Ed. Engl*., 3, 442.

65. Huisgen, R., Konz, W. E., Gream, G. E. Evidence for different valence tautomers of bromocyclooctatetraene. 1970, *J. Am. Chem. Soc*., 92, 4105.

66. Torres, E., Duque, M. D., Vanderlinden, E., Ma, C., Pinto, L. H., Camps, P., Froeyen, M., Vázquez, S., Naesens, L. Role of the viral hemagglutinin in the anti-influenza virus activity of newly synthesized polycyclic amine compounds. 2013, *Antiviral Res.* 99, 281.

67. Kolocouris, A., Tzitzoglaki, C., Johnson, F. B., Zell, R., Wright, A. K., Cross, T. A., Tietjen, I., Fedida, D., Busath, D. D. Aminoadamantanes with persistent in vitro efficacy against H1N1(2009) influenza A. 2014, *J. Med. Chem.*, 57, 4629.

68. Cady, S. D., Mishanina, T. V., Hong, M. Structure of amantadine-bound M2 transmembrane peptide of influenza A in lipid bilayers from magic-angle-spinning solid-state NMR: the role of Ser31 in amantadine biding. 2009, *J. Mol. Biol.*, 385, 1127.

69. Wu, Y., Canturk, B., Jo, H., Ma, C., Gianti, E., Klein, M. L., Pinto, L. H., Lamb, R. A., Fiorin, G., Wang, J., DeGrado, W. F. Flipping in the pore: discovery of dual inhibitors that bind in different orientations to the wild-type versus the

amantadine-resistant S31N mutant of the influenza A virus M2 proton channel. 2014, *J. Am. Chem. Soc.*, 136, 17987.

70. Wang, J., Ma, C., Fiorin, G., Carnevale, V., Wang, T., Hu, F., Lamb, R. A., Pinto, L. H., Hong, M., Klein, M. L., DeGrado, W. F. Molecular dynamics simulation directed rational design of inhibitors targeting drug-resistant mutants of influenza A virus M2. 2011, *J. Am. Chem. Soc.*, 133, 12834.

71. Kolocouris, A., Tataridis, D., Fytas, G., Mavromoustakos, T., Foscolos, G. B., Kolocouris, N., De Clercq, E. Synthesis of 2-(2-adamantyl)piperidines and structure anti-influenza virus A activity relationship study using a combination of NMR spectroscopy and molecular modeling. 1999, *Bioorg. Med. Chem. Lett*., 9, 3465.

72. Kolocouris, N., Zoidis, G., Foscolos, G. B., Fytas, G., Prathalingham, S. R., Kelly, J. M., Naesens, L., De Clercq, E. Design and synthesis of bioactive adamantane spiro heterocycles. 2007, *Bioorg. Med. Chem. Lett.*, 17, 4358.

73. Kolocouris, A., Spearpoint, P., Martin, S. R., Hay, A. J., Lopez-Querol, M., Sureda, F. X., Padalko, E., Neyts, J., De Clercq, E. Comparisons of the influenza virus A M2 channel binding affinities, anti-influenza virus potencies and NMDA antagonistic activities of 2-alkyl-2-aminoadamantanes and analogues. 2008, *Bioorg. Med. Chem. Lett*., 18, 6156.

74. Barniol-Xicota, M., Gazzarrini, S., Torres, E., HU, Y., Wang, J., Naesens, L., Moroni, A., Vázquez, S. Slow but Steady Wins the Race: Dissimilarities among New Dual Inhibitors of the Wild-Type and the V27A Mutant M2 Channels of Influenza A Virus. 2017, *J. Med. Chem.* 60, 3727.

75. Togo, H., Aoki, M., Kuramochi, M., Yokoyama, M. Radical decarboxylative alkylation onto heteroaromatic bases with trivalent iodine compounds. 1993, *J. Chem. Soc., Perkin Trans.* 1, 2417.

76. Gu, R.-X., Liu, L. A., Wang, Y.-H., Xu, Q., Wei, D.-Q. Structural comparison of the wild-type and drug-resistant mutants of the influenza A M2 proton channel by molecular dynamics simulations. 2013, *J. Phys. Chem. B*, 117, 6042.

77. Gu, R.-X., Liu, L. A., Wei, D.-Q. Structural and energetic analysis of drug inhibition of the influenza A M2 proton channel. 2013, *Trends Pharm. Sci.*, 34, 571.

78. Gu, R.-X., Liu, L. A., Wei, D. Drug inhibition and proton conduction mechanisms of the influenza A M2 proton channel. 2015, *Adv. Exp. Med. Biol.*, 827, 205.

79. Van Nguyen, H., Nguyen, H. T., Le, L. T. Investigation of the free energy profiles of amantadine and rimantadine in the AM2 binding pocket. 2016, *Eur. Biophys. J.*, 45, 63.

80. Llabrés, S., Juárez-Jiménez, J., Masetti, M., Leiva, R., Vázquez, S., Gazzarrini, S., Moroni, A., Cavalli, A., Luque, F. J. Mechanism of the pseudoirreversible binding of amantadine to the M2 proton channel. 2016, *J. Am. Chem. Soc.*, 138, 15345.

81. Liang, R., Swanson, J. M. J., Madsen, J. J., Hong, M., DeGrado, W. F., Voth, G. A. Acid activation mechanism of the influenza A M2 proton channel. 2016, *Proc. Natl. Acad. Sci. USA*, 113, E6955.

82. Fu, R., Miao, Y., Qin, H., Cross, T. A. Probing hydronium ion histidine NH exchange rate constants in the M2 channel via indirect observation of dipolar-dephased ^{15}N signals in magic-angle-spinning NMR. 2016, *J. Am. Chem. Soc.* 138, 15801.

83. Jeong, B.-S., Dyer, R. B. Proton transport mechanism of M2 proton channel studied by laser-induced pH jump. 2017, *J. Am. Chem. Soc.* 139, 6621.

84. Lin, C.-W., Mensa, B., Barniol-Xicota, M., DeGrado, W. F., Gai, F. Activation pH and gating dynamics of influenza A M2 proton channel revealed by single-molecule spectroscopy. 2017, *Angew. Chem. Int. Ed.*, 56, 5283.

85. Mandala, V. S.; Liao, S. Y., Kwon, B., Hong, M. Structural basis for asymmetric conductance of the influenza M2 proton channel investigated by solid-state NMR spectroscopy. 2017, *J. Mol. Biol.,* 429, 2192.

86. Thomaston, J. L., Alfonso-Prieto, M., Woldeyes, R. A., Fraser, J. S., Klein, M. L., Fiorin, G., DeGrado, W. F. High-resolution structures of the M2 channel from influenza A virus reveal dynamic pathways for proton stabilization and transduction. 2015, *Proc. Natl. Acad. Sci. USA*, 112, 14260.

87. Thomaston, J. L., DeGrado, W. F. Crystal structure of the drug-resistant S31N influenza M2 proton channel. 2016, *Protein Sci.*, 25, 1551.

88. Hu, Y., Musharrafieh, R., Ma, C., Zhang, J., Smee, D. F., DeGrado, W. F., Wang, J. An M2-V27A channel blocker demonstrates potent in vitro and in vivo antiviral activities against amantadine-sensitive and –resistant influenza A viruses. 2017, *Antiviral Res.*, 140, 45.

89. Li, F., Ma, C., DeGrado, W. F., Wang, J. Discovery of highly potent inhibitors targeting the predominant drug-resistant S31N mutant of the influenza A virus M2 proton channel. 2016, *J. Med. Chem.*, 59, 1207.

90. Ma, C., Zhang, J., Wang, J. Pharmacological characterization of the spectrum of antiviral activity and genetic barrier to drug resistance of M2-S31N channel blockers. 2016, *Mol. Pharmacol.*, 90, 188.

91. Li, F., Hu, Y., Wang, Y., Ma, C., Wang, J. Expeditious lead optimization of isoxazole-containing influenza A virus M2-S31N inhibitors using the Suzuki-Miyaura cross-coupling reaction. 2017, *J. Med. Chem.*, 60, 1580.

92. Tzitzoglaki, C., Wright, A., Freudenberger, K., Hoffmann, A., Tietjen, I., Stylianakis, I., Kolarov, F., Fedida, D., Schmidtke, M., Gauglitz, G., Cross, T. A., Kolocouris, A. Binding and proton blockage by amantadine variants of the influenza M2$_{WT}$ and M2$_{S31N}$ explained. 2017, *J. Med. Chem.*, 60, 1716.

93. Hu, Y., Wang, Y., Li, F., Ma, C., Wang, J. Design and expeditious synthesis of organosilanes as potent antivirals targeting multidrug-resistant influenza A viruses. 2017, *Eur. J. Med. Chem.*, 135, 70.

94. Nguyen, J. T., Smee, D. F., Barnard, D. L., Julander, J. G., Gross, M., de Jong, M. D., Went, G. T. Efficacy of Combined Therapy with Amantadine, Oseltamivir, and Ribavirin In Vivo against Susceptible and Amantadine-Resistant Influenza A Viruses. 2012, *PLoS One*, 7, e31006.

95. Seo, S., Englund, J. A., Nguyen, J. T., Pukrittayakamee, S., Lindegardh, N., Tarning, J., Tambyah, P. A., Renaud, C., Went, G. T., de Jong, M. D., Boeckh, M. Combination therapy with amantadine, oseltamivir and ribavirin for influenza A infection: safety and pharmacokinetics. 2013, *J. Antivir. Ther.*, 18, 377.
96. Li, F., Ma, C., Wang, J. Inhibitors targeting the influenza virus hemagglutinin. 2015, *Curr. Med. Chem.*, 22, 1361.